Original Paper

Cellular Physiology and Biochemistry

Cell Physiol Biochem 2010;26:147-154

Accepted: July 05, 2010

Phosphoglycerate Kinase 1 Promoting Tumor Progression and Metastasis in Gastric Cancer - Detected in a Tumor Mouse Model Using Positron Emission Tomography/Magnetic Resonance Imaging

Derek Zieker[1,2,*], Ingmar Königsrainer[1,*], Jürgen Weinreich[1], Stefan Beckert[1], Jörg Glatzle[1], Kay Nieselt[3], Sarah Bühler[2], Markus Löffler[1,2], Jochen Gaedcke[4], Hinnak Northoff[2], Julia G. Mannheim[5], Stefan Wiehr[5], Bernd J. Pichler[5], Claus von Weyhern[6], Björn L.D.M. Brücher[1] and Alfred Königsrainer[1]

[1]Department of General, Visceral and Transplant Surgery, Comprehensive Cancer Center, University of Tuebingen, [2]Institute of Clinical and Experimental Transfusion Medicine, University of Tuebingen, [3]Department of Information and Cognitive Sciences, Center for Bioinformatics University of Tuebingen, [4]Department of General, Visceral and Transplant Surgery, University of Goettingen, [5]Department of Radiology, Laboratory for Preclinical Imaging and Imaging Technology of the Werner Siemens-Foundation, University of Tuebingen, [6]Department of Pathology, University of Tuebingen, *The first two authors contributed equally to this work

Key Words

PGK1 • CXCR4 • Peritoneal carcinomatosis • Cancer dissemination • Metastasis • Gastric cancer • Cancer imaging • PET/MRI

Abstract

Background/Aims: Tumor dissemination is frequent in gastric cancer and implies a poor prognosis. Cure is only achievable provided an accurate staging is performed at primary diagnosis. In previous studies we were able to show a relevant impact of increased phosphoglycerate kinase 1 expression (PGK1; a glycolytic enzyme) on invasive properties of gastric cancer *in-vivo* and *in-vitro*. Thus the aim of the present study was to evaluate the effect of enhanced PGK1 expression in gastric cancer employing magnetic resonance (MR)-imaging combined with positron emission tomography (PET), a recently emerging new high resolution imaging technique in a mouse model. Methods: A metastatic nude mouse model simulating human gastric cancer behavior by orthotopic tumor implantation was established. Mice were divided into one control group (n=5) and two experimental groups (n=30) divided by half in animals baring tumors from MKN45-cells and MKN45-cells with plasmid-mediated overexpression of PGK1. In the course of tumor growth MR-imaging and PET/MRI fusion was performed. Successively experimental animals were examined macroscopically and histopathologically regarding growth, metastasis and PGK1 expression. Results: Elevated PGK1 expression increased invasive and metastatic behavior of implanted gastric tumors significantly. MR/PET- imaging results *in-vivo* and subsequent *ex-vivo* findings concerning tumor growth and metastasis correlated excellently and could be underlined by concordant immuohistoche-

KARGER

Fax +41 61 306 12 34
E-Mail karger@karger.ch
www.karger.com

1015-8987/10/0262-0147$26.00/0

Accessible online at:
www.karger.com/cpb

Dr. Derek Zieker
Dept General Visceral and Transplant Surgery, Comprehensive Cancer Center
University of Tuebingen, Hoppe-Seyler-Strasse 3, 72076 Tuebingen (Germany)
Tel. +49-7071-2981658, Fax +49-7071-295459,
E-Mail derek.zieker@med.uni-tuebingen.de

mical PGK1 staining. Conclusion: Consistent *in-vivo* findings suggest that PGK1 might be crucially involved in gastric malignancy regarding growth and metastasis, which was also underlined by novel imaging techniques. Thus, PGK1 may be exploited as a prognostic marker and/or be of potential therapeutic value preventing malignant dissemination.

Introduction

Gastric cancer combined with peritoneal carcinomatosis or metastasis is associated with a poor prognosis [1, 2]. Currently, an effective therapy is lacking and the five-year survival rate is below 2 % [3]. A curative therapeutic intent can only be undertaken in early stages by multimodal treatment including radical resection which requires accurate staging at primary diagnosis with potent imaging tools. Among those promising options is computed tomography (CT), magnetic resonance (MR) and positron emission tomography (PET)-imaging. To date non invasive early detection of tumor spreading in patients with peritoneal carcinomatosis remains challenging even with latest progress in imaging technology [4]. Although contrast enhanced CT is currently the gold standard for diagnosis and staging, recent clinical studies have indicated that CT combined with Fluordeoxyglucose PET ([^{18}F]DG–PET) can improve tumor detection and serve for therapeutic response monitoring [5, 6]. At present CT-imaging offers only limited soft tissue contrast [7] and its appliance involves high radiation exposure and great nephrotoxicity [8]. Even when employing PET imaging [^{18}F]DG is not always capable of providing a sufficient tumor-to-background-ratio. Aware of the fact that MR-imaging quality suffers from gut motion and breathing artifacts, it never the less seems to be a potent tool in closing the indicated CT-imaging-gap and thus may provide essential advantages in tumor detection combining omitted radiation exposure with low nephrotoxic impact. For evaluation of non-invasive imaging of tumorigenesis and therapy response, MR-imaging in small animal models is of major interest. However, detailed *in-vivo* studies in animals concerning the correlation between imaging results and malignant dissemination are missing still.

Researching features that enable gastric tumors to metastasize we encountered phosphoglycerate kinase 1 (PGK1) to be a crucially involved molecule [9]. PGK1 is an ATP-generating enzyme in the glycolytic pathway catalyzing the conversion of 1,3-diphosphoglycerate to 3-phosphoglycerate and further affects DNA replication and repair [10]. With regard to tumorigenesis it is assumed that genes involved in the glycolytic pathway are expressed increasingly to provide solid tumor cells with ATP when their supply of oxygen is limited [11]. PGK1 is known to be involved in the onset of several malignancies, such as prostate, breast, pancreatic cancer and multi-drug resistant ovarian cancer [9, 10, 12-14]. In patients suffering from gastric cancer with peritoneal carcinomatosis we recently detected an overexpression of PGK1 [9]. We were able to show a direct connection between PGK1 signaling and the chemokine receptor CXCR4 [15]. Nevertheless, the lately most striking finding was that PGK1 seems to be the central molecule concerning tumor invasion and tumor growth in gastric cancer cells *in vitro*.

To further elucidate the role of PGK1 *in-vivo* and to find an imaging tool that is able to detect tumor growth and dissemination sufficiently, we established a metastatic gastric cancer animal model by orthotopic implantation of tumor tissue onto the serosa of nude mice. Regarding the disadvantages of CT-imaging we decided to combine MR-imaging and [^{18}F]DG-PET. Thus this study was designed to assess the impact of elevated PGK1 expression on metastasis and tumor growth.

Materials and Methods

Cell culture

The human gastric adenocarcinoma cell line MKN45 was purchased (German Collection of Microorganisms and Cell Cultures, Braunschweig, Germany) and cultured in RPMI 1640 medium supplemented with 20% fetal bovine serum gold (Lonza, Basel, Switzerland).

PGK1 overexpression performed by transfection

A plasmid mediated transfection was performed using the plasmid vector pEF-IRES containing *PGK1*. Briefly, 6 x 10^5 MKN45 cells were seeded in 24 well plates one day before transfection. Cells were transfected employing Tfx-50 (Promega, Madison, USA) and 1 µg plasmid DNA was administered per well. The empty vector pEF-IRES was transfected, serving as a negative control. Transfected cells were selected by 5 µg/ml Puromycin (AppliChem, Darmstadt, Germany) 24 h after transfection [15, 16].

Experimental animals

Thirty-five female HsdCpb:NMRI-Foxn1nu nude mice eight weeks of age, weighing 30 (29 - 32) g, were purchased (Harlan Winkelmann GmbH, Borchen, Germany) and raised under specific pathogen free conditions for one week to adapt to the surroundings before initiating the experiment. All animals were maintained on a daily 12 hour light/12 hour dark cycle and were supplied with unlimited food and water. The facility and

the protocol for the experiments were consistent with the regulations on animal use for research according to federal law and approved by the local animal care committee.

Tumor tissues and histological assessment

In five donor animals each per group (MKN45/PGK1-MKN45), 0.2 ml of cell suspension (4 x 10^6 cells) in phosphate buffered saline (PBS) was subcutaneously injected into the right flank of nude mice to form the entity of a solid cancer. After tumor growth to a diameter of 1.4 cm, nude mice were sacrificed for tumor dissection. Tumors were removed, necrotic tissue was dislodged and the remaining vital tumor tissue was cut into pieces using scissors. Each tumor piece was weighed using a Sartorius type R 180 D balance (Sartorius AG, Goettingen, Germany) and adjusted to 150 (147 - 154) mg. The tumor pieces were kept in RPMI 1640 medium supplemented with 10 % fetal calf serum (FCS), 100 U/ml penicillin and 100 U/ml streptomycin, for subsequent use. Pieces of fresh tumor tissue were stored in liquid nitrogen or used subsequently for orthotopic implantation. The tumors from donor mice yielded sufficient tissue for xeno-transplanting a 150 mg piece from every animal to two experimental animals subsequently. All tissue obtained from donor mice and used in the experiments was histopathologically examined at the University department of pathology.

Animal model

The metastatic mouse model simulating the behavior of human gastric cancer was established by orthotopic implantation of histologically intact human tumor tissue onto the gastric serosa of nude mice. Mice were randomly divided into three groups: control group (n=5), MKN45-gastric cancer group (n=15) and plasmid-mediated overexpression of PGK1-MKN45-gastric cancer group (n=15, one animal lost in follow up => (n=14)). While the control group received only a suture on the stomach wall, the other two experimental groups received a piece of tumor derived either from the plasmid-mediated overexpression of PGK1-MKN45 cells or from the native MKN-45 cells. Mice were anesthetized with 100 mg ketamine per kg body weight and 5 mg xylazine per kg body weight and the abdominal skin was cleaned with Softasept N (Braun, Melsungen, Germany). An incision was performed cutting through the left upper abdominal pararectal line and the peritoneum. The stomach wall was carefully exposed, and a part of the serosal membrane in the middle of the greater curvature of the glandular stomach was mechanically injured using scissors. A tumor piece of 150 mg was subsequently fixed to each injured side of the serosal surface with a 6-0 Prolene (Ethicon GmbH, Norderstedt, Germany) suture. The stomach was then returned to the peritoneal cavity, and the abdominal wall and the skin was closed with 6-0 and 5-0 Prolene sutures. The whole procedure was performed following the doctrine of aseptic manipulation.

MR and PET-MR-imaging

PET imaging was performed using an Inveon dedicated small animal PET scanner (Siemens Preclinical Solutions, Knoxville, TN, USA). The scanner yields a spatial resolution of about 1.4 mm in the reconstructed image and has a 12 cm axial field of view (FOV) covering an entire mouse at one bed position. PET data were acquired in list mode and an iterative ordered-subset expectation maximization algorithm (OSEM2D) was used for image reconstruction. According to our standard PET imaging protocols attenuation correction was not performed on mice. MR-imaging was performed on a 7 T small animal MR scanner (ClinScan, Bruker Biospin MRI, Ettlingen, Germany), equipped with a 300 mm bore magnet, a gradient system with an inner diameter of 200 mm which operates under the syngo MRI software (Siemens Medical Solutions, Germany) for image acquisition. A 35 mm transmit-receive whole body mouse coil (Bruker BioSpin MRI) was installed in the isocenter of the MR scanner. A T2 weighted 3D turbo spin echo (tse) sequence was applied with a FOV of 57 mm in read direction and 62.5 % in phase direction. This 3D sequence with a repetition time (TR) of 3000 ms and an echo time (TE) of 205 ms yielded an isotropic resolution of 0.22 mm. 10 animals each from the two cancer baring experimental groups and 5 control animals were investigated at day 20 and, subsequently, at day 30 after tumor implantation. The animals were anaesthetized by an isoflurane/oxygen mixture (1.5% isoflurane, 0.8L/min oxygen). All mice were kept anesthetized during tail vein injection of 12.5 MBq [^{18}F]DG and during PET and MR imaging. However, during the 55 min tracer uptake period the animals were conscious to avoid increased non-specific intestinal tracer uptake. After the tracer uptake period, the animals were placed on an animal bed at the center FOV of the PET scanner. After a 10 min static PET acquisition, the animals were transferred on their beds to the MR-imaging scanner. Rigid fusion of PET and MR-images was performed using Inveon Research Workplace software (Siemens Preclinical Solutions, Knoxville, TN, USA). Statistical analysis of the *in-vivo* imaging data was performed with Origin software version 8.0.

Ex-vivo evaluation of growth and metastasis

42 days after tumor implantation all mice were sacrificed by cardiac puncture following bleeding to death under anesthesia. Autopsies were performed immediately and the tumors on the stomach wall removed, assessed, weighed and examined histologically. Mice exhibiting no tumor engraftment were excluded from all further experiments (one loss in the plasmid-mediated overexpression of PGK1-MKN45-gastric cancer group). The lungs, livers, and other peritoneal organs were processed histologically for assessment of metastases after careful macroscopic examination.

Mice were initially macroscopically assessed based on local findings, including protrusion and palpable tumor mass. Primary tumors on the stomach wall were investigated and weighted after excision using a balance (Sartorius type R 180 D, Sartorius AG, Goettingen, Germany). A tumor index as the ratio of primary tumor weight to animal weight in percent was calculated (primary tumor weight/animal weight x100). Peritoneal area affected by metastatic growth was assessed planimetrically using GSA Image Analyzer V.3.3.3 software (GSA software, Rostock, Germany), a digitizer board and transparent OpSite Flexigrid film (Smith & Nephew; London, UK) for assignment. Weight of total peritoneal metastases was assessed based on

the assumption of the mean weight of peritonea obtained from control mice (n=5) as a calibrator and the increased weight was attributed to metastatic peritoneal growth. Quantities of metastases observed in organs most frequently affected by metastatic growth were assessed.

Histopathological examinations

All tumor tissue from donor mice and *xeno*-transplanted animals used in these experiments was classified by histopathological examination at the department of pathology at Tuebingen University. Xenografts of tumor tissue and organs involved in metastatic processes were fixed in 5 % phosphate buffered formalin, embedded in paraffin, sectioned to 2 µm slides, and stained with hematoxylin/eosin.

Immunohistochemistry

For immunohistochemical examination, 2 µm tissue slides from formalin fixed, paraffin embedded tumor tissue were used. In brief, sections were deparaffined in xylene, rehydrated, and epitope retrieval was performed in citrate buffer (pH 6) using the Pascal pressure chamber (Dako, DakoCytomation GmbH, Hamburg, Germany) for 2 minutes at 125°C. After blocking endogenous peroxidases with 3% H_2O_2, PGK1/2 primary antibody (dilution 1:200; clone: sc-48342; Santa Cruz Biotechnology Inc., Santa Cruz, CA, USA) was incubated for 60 minutes. Detection was carried out using Envision™ goat-anti-mouse secondary antibody (Dako, DakoCytomation GmbH, Hamburg, Germany) for 60 minutes followed by incubation with diaminobenzidine (DAB). Nuclear as well as cytoplasmic staining was considered specific, and a moderate to strong expression was considered positive [15].

Statistical analyses

Normality testing was performed using the Kolmogorov-Smirnov test. Statistical analysis was subsequently performed applying Student's t-test and Wilcoxon rank-sum test (Mann-Whitney U test), where adequate. A p-value of < 0.05 was considered significant. Results are documented as median [min-max] or percent of total where applicable.

Results

Histopathological examinations

All tumor tissue used experimentally and obtained from donor mice in the course of these investigations was further evaluated by histopathological examination at the department of pathology at Tuebingen University and confirmed by accordant pathological findings. All animals survived the surgical procedures.

MR and PET-MR-imaging of gastric cancer

Radiological evaluation was performed 20 and, subsequently, 30 days after tumor implantation (Fig. 1B). Images from sham treated animals did not show any malignant alterations. MR volumetry revealed a significant increase in tumor volume of PGK1-MKN45 mice in the time course. 20 days after tumor implantation a tumor volume of 452 ± 288 mm^3 was detected which increased to 1630 ± 302 mm^3 in the following 10 days (p=0.00001). The MKN45 group showed an increase of tumor volume from 412 ± 270 mm^3 at day 20 to 963 ± 153 mm^3 after 30 days (p=0.019) (Fig. 1A). 30 days after implantation, the tumor-tissue of PGK1-MKN45 mice was 59% larger in size compared to the MKN45 group, comparing the volumetry data of both groups, this difference resulted statistically significant (p=0.0045) (Fig. 1A+1B). PET-MR-images showed an increased uptake of [^{18}F]DG at the tumor site (Fig. 2). However, for better anatomy, fusion with MR-images increased specificity.

Ex-vivo evaluation of growth and metastasis of orthotopically implanted tumors

42 days after tumor *xeno*-transplantation, all mice were sacrificed by cardiac puncture. Autopsies were performed immediately. One mouse of the PGK1-MKN45-gastric cancer group had to be excluded due to missing tumor engraftment. Comparing the results obtained after autopsy of mice from the MKN45-gastric cancer group (n=15) and plasmid-mediated overexpression of PGK1-MKN45-gastric cancer group (n=14) the following findings were obtained: By primary macroscopical assessment of the animals the amount of macroscopically visible tumor mass appeared higher in the PGK1-MKN45-gastric cancer group. Assessing detected metastases, primary tumor weight and peritoneal surface covered by malignant tissue, the PGK1-MKN45-gastric cancer group showed a significantly elevated amount of metastases ($p<0.05$) compared with the MKN45-gastric cancer group (Table 1). The gain of peritoneal weight attributed to growth of metastatic tissue was significantly elevated in the PGK1-MKN45-gastric cancer group (p=0.032) (Table 1) and the peritoneal area covered by metastases (p=0.005) was significantly increased, whereas animal weight was highly comparable (p=0.542). This finding accordingly resulted in a significantly elevated tumor index, as a function of percental primary tumor weight to total weight of the animal. Evaluating the metastatic potential into solid organs, such as liver, spleen and colon, we detected significant differences between the two groups. All animals showed metastasis at the peritoneal surface and/or in distant organs which renders the animal groups comparable and is a sign for the aggressiveness of the tumor cells line (p=0.5). More metastases were observed

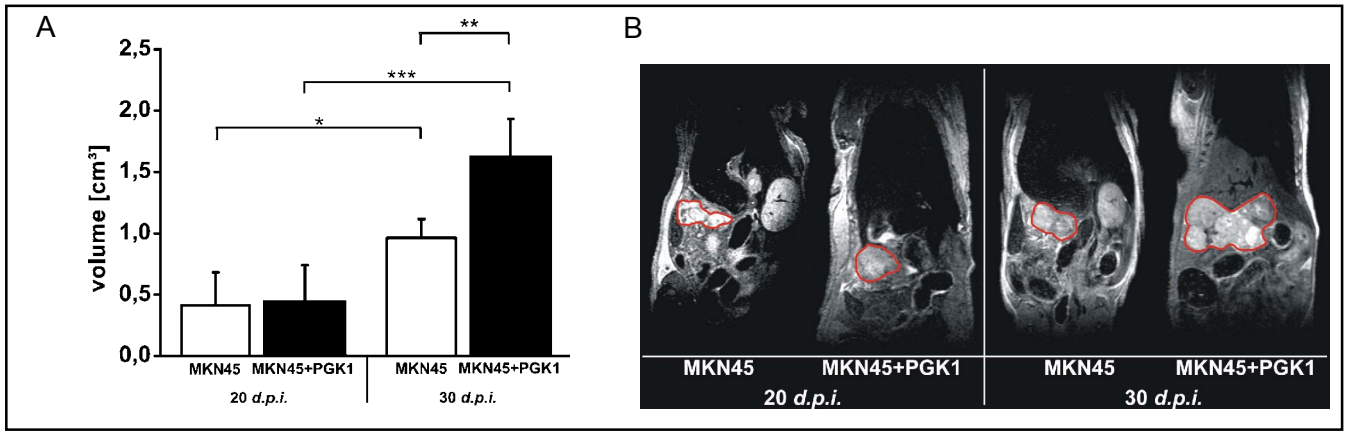

Fig. 1. MR-imaging. 1A: MR volumetry of MKN45 and MKN45+PGK1 cancer tissue in mice (n=10) twenty days and 30 days after tumor implantation (d.p.i.). Tumor volumes are given in mm^3 and significant differences ($p<0.05$) are shown and marked by asterisks. Statistical analysis was performed employing Student´s t-test (2-tailed) and data are given as means ± standard deviation. (* p=0.019/** p=0.0045/*** p=0.00001). 1B: MR-images of mice bearing MKN45 and MKN45+PGK1 tumors 20 days after implantation (left) and 30 days after implantation (right). Red marks indicate the tumor mass.

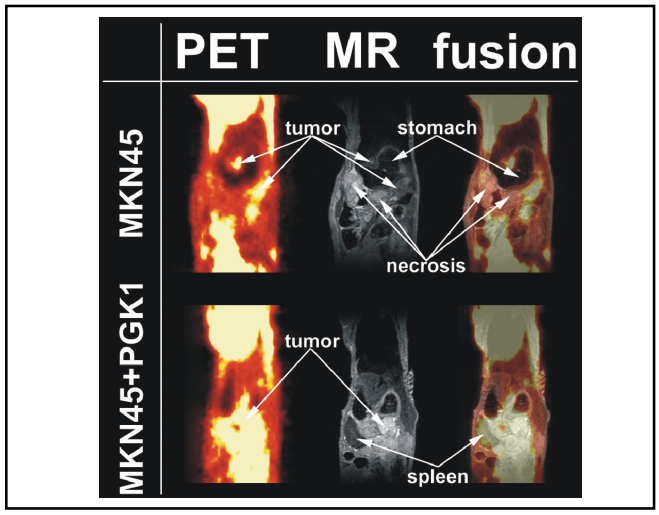

Fig. 2. PET-MR-imaging. Small animal PET images (left column), MR images (center column) and fused PET/MR images (right column) of mice bearing MKN45 tumors (upper row) and MKN45+PGK1 tumors (lower row) 30 days after implantation.

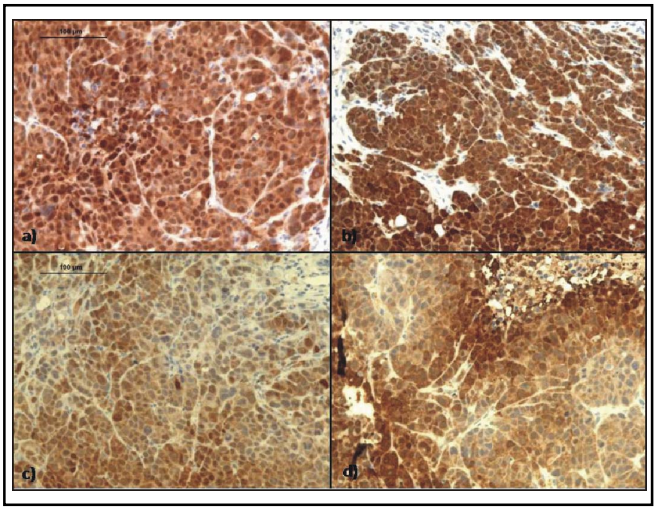

Fig. 3. Immunohistochemistry after autopsy to explore PGK1 expression. Immunohistochemical staining was performed after autopsy to explore PGK1 expression in tumor engrafted mice. PGK1-MKN45-gastric cancer group (a and b) and MKN45-gastric cancer group (c and d). PGK1-MKN45-gastric cancer group showed a homogeneous strong nuclear and moderate cytoplasmic staining for PGK1 (a and b), whereas only a weak to moderate staining in tumor cells of MKN45-gastric cancer group (c and d) was detected. Enhanced staining was observed adjacent to necrotic tumor cells (d). All images are 500-times magnified, the graduation marks shown depict a distance of 100 µm.

in the PGK1-MKN45-gastric cancer group compared to the MKN45-gastric cancer group. The total metastatic burden accounted as the total amount of distant metastases was significantly higher in animals baring PGK1-MKN45-tumors (70 vs. 22; p=0.005) as well as in distinct organs (liver (p<0.001), spleen (p=0.003) and colon (p=0.008) whereas the difference in dissemination to the intestine was not significant. Liver metastases were found exclusively in the PGK1-MKN45-gastric cancer group (metastases found in 50% of animals), and accounted for more metastases in spleen (metastases found in 57% vs. 33% of animals) and colon (metastases

found in 64% vs. 26% of animals) compared to the MKN45-gastric cancer group (Table 1). No alterations were detected in any of the sham treated animals.

Immunohistochemistry

Immunohistochemical staining was performed after autopsy confirming PGK1 expression in tumor engrafted mice. The PGK1-MKN45-gastric cancer group showed a homogeneously strong nuclear and a moderate cytoplasmic staining for PGK1. In contrast the MKN45-gastric cancer group revealed only a weak to moderate staining in the vast majority of cells. In addition, most cells adjacent to necrotic tumor cells showed a strong staining pattern (Fig. 3).

Data by *ex- vivo* evaluation	PGK1-MKN45-gastric cancer (n=14)	MKN45-gastric cancer (n=15)	p- value
Animal weight (g)	28.00 [22.00-32.0]	28.45 [21.91-32.3]	0.542
Primary tumor weight (g)	3.15 [1.20-5.21]	2.34 [0.70-3.98]	0.009
Tumor Index (%)	11.35 [4.58-21.55]	7.9 [2,5-13.20]	0.008
Peritoneal area affected by tumor lesions (mm^2) #	300.78 [118.89-452.22]	62.36 [0-161.02]	0.005
Peritoneal weight gain (g) #	1.04 [0.16-2.06]	0.15 [0.01-0.45]	0.032 ‡
Metastasis (n/total; %)	14/14 (100%)	15/15 (100%)	0.5
Metastatic burden (n)	70	22	0.005 ‡
Affected animals (n/total; %)	12/14 (86%)	11/15 (73%)	
Metastases (n)			
Liver (n/total; %)	7/14 (50%) [0-5]	0/15 (0%)	<0.001‡
Spleen (n/total; %)	8/14 (57%) [0-6]	5/15 (33%) [0-1]	0.003 ‡
Intestine (n/total; %)	12/14 (86%) [0-7]	9/15 (60%) [0-4]	0.203 ‡
Colon (n/total; %)	9/14 (64%) [0-5]	4/15 (26%) [0-1]	0.008 ‡

Table 1. The table shows *ex-vivo* results assessing differences between mice bearing tumors overexpressing PGK1 (PGK1-MKN45-gastric cancer) and mice bearing native MKN45 induced orthotopic gastric tumors (MKN45-gastric cancer). Weight of animals and weight of primary tumors at the site of implantation is given, as well as a tumor index (as a percent ratio of primary tumor to animal weight). Further the peritoneal area involved in metastatic process is given after planimetrical assessment. The increase in peritoneal weight and the peritoneal surface area covered by tumors, calculated using controls as a calibrator is given (n=5 for each group; marked by #). The number of animals affected by metastasis is given as numbers of total animals and in percent as well as related to different organs. The amount of metastases determined in liver, spleen, intestine and colon are shown in square brackets as minimum-maximum ranges observed in different animals. Furthermore the metastatic burden, which is the total number of metastases detected in distant organs in all animals, is given as well as the numbers of animals affected. Differences in between groups (PGK1-MKN45-gastric cancer vs. MKN45-gastric cancer) were assessed after normality testing by Kolmogorov-Smirnov test applying Student's t-test and Wilcoxon rank-sum test (marked by ‡), where adequate. When applicable, medians are given with minimum- maximum range in square brackets or percentage of total in brackets. An inter-group difference below 0.05 was considered statistically significant.

Discussion

The aim of this study was to investigate the impact of elevated PGK1 expression on gastric cancer growth and metastasis *in-vivo*. Although gastric cancer is a leading cause of global disease and mortality and frequently associated with metastasis and peritoneal dissemination [1, 2], the complex underlying mechanisms for malignant spreading are not clearly investigated yet. Recently, the glycolytic enzyme PGK1 has been determined as a crucial factor for dissemination of gastric cancer, constituting a novel link to dissemination in gastric cancer and other malignancies [9, 15]. Therefore a metastatic mouse model simulating human gastric cancer behavior by orthotopic implantation of human histologically proven tumor tissue onto the gastric serosa of nude mice was established. For exact continuous *in-vivo* monitoring of tumor progression and spreading MR and PET-MR-imaging were chosen, followed by sectioning of animals with subsequent histological examination. The main findings of this study revealed a significantly increased invasive growth pattern and metastatic rate in mice after implantation of tumors overexpressing PGK1. It is documented that MKN45 cells exhibit an aggressive metastatic behavior in nude mice [17], which we can confirm due to the fact, that all mice were affected by metastatic growth. The importance of our findings can be underlined by the fact that after 20 days both experimental groups did not show significant differences in MR-volumetry, whereas after 30 days and *ex-vivo* significant differences between the two groups were substantiated. Metastases were significantly more frequent in mice with tumors expressing elevated levels of PGK1. In addition liver metastases were exclusively detected in these animals. Further peritoneal carcinomatosis also showed a significantly greater extent in the PGK1 overexpressing animals. Thus, our results are concordant with the clinical findings of aggressive gastric cancers in humans and underline the impact of our metastatic model simulating human gastric cancer. Immunohistological assessment additionally revealed an

overexpression of PGK1 in the primary tumors and metastasized tissues of these animals, confirming former results obtained from *in-vitro* studies evaluating PGK1 [15]. Although MKN45 cells do already have a highly aggressive potential in-vivo [17], the altered metastatic profile and the tumor promoting impact observed in our study can be related to PGK1 overexpression. In previous studies we detected a difference in PGK1 mRNA expression in patients with and without peritoneal carcinomatosis of corresponding TN-stages accounting to 4.6-fold [9]; this is in the range of mRNA levels observed in MKN45-PGK1 cells as described previously, varying from 4 to 5-fold [15]. Thus the differences between gastric cancers in humans disseminating to the peritoneum and tumors that do not disseminate and those in our orthotopic *xeno*-transplanted *in-vivo* mouse model can be assumed fairly comparable, at least regarding PGK1 mRNA expression.

Cancer tissue is constantly striving to expand itself, either via local tumor growth or via dissemination. Both mechanisms depend on an increasing energy supply. Nowadays, it is widely accepted and multiply shown that solid tumor cells employ glycolytic enzymes such as PGK1 for ATP production [11]. Already in the 1950s Otto Warburg was able to show an increased dependence on glycolysis as a source of energy in ascitic cancer cells assuming an impaired mitochondrial function [18]. Previous findings substantiated the notion that PGK1 could be essentially involved in dissemination of gastric cancer, as PGK1 overexpressing gastric cancer tissue showed significantly elevated tumor invasion, tumor growth and a higher metastatic rate in comparison to corresponding tumor tissue without overexpression of PGK1 [9, 15]. Thus delineating findings from our previous studies documenting elevated PGK1 levels in patients suffering from peritoneal carcinomatosis induced by gastric cancer and the subsequent assessment of the role of PGK1 in gastric cancer cells and its regulations *in-vitro* [9, 15], in this study we are able to prove an impact of PGK1 in gastric cancer biology *in-vivo*.

Furthermore we were able to correlate metastasis and peritoneal dissemination via *in-vivo* PET/MR-imaging, assessing a novel diagnostic technique in gastric cancer. As gastric cancer is only curable by radical resection, adequate staging employing high-resolution imaging tools is a crucial factor. Based on our findings concerning the correlation between histopathological findings and imaging results, PET/MR imaging proves an advantageous supportive technique. Consequently, when comparing CT imaging to MRI, the latter provides superior soft-tissue contrast and enables image acquisition in any orientation, which therefore increases probability of metastasis detection. Furthermore functional data are implied by PET-MRI imaging, apart from morphological information provided by CT and MR-imaging only, which is of high complementary value for metastasis detection [7]. Besides risks induced by radiation and CT contrast agents are negligible in this setting, which may be of further value when dealing with multi-morbid patients [8]. In synopsis PET-MRI should yield higher accuracy and therefore a more exact TNM staging is feasible than currently available techniques such as PET-CT or whole body MRI can provide [7] and therefore the technique might help reaching a new level in clinical oncology and research. Although comprising relevant advantages compared to conventional techniques as the current standard method computed tomography, there is still some potential to improve the method. A means for further improvement is simultaneous PET-MR imaging enhancing spatial overlay, diagnostic accuracy and reducing uncertainties from intestinal peristalsis, especially when detecting very small lesions or metastases [19].

In summary the findings of this study underline the evidence that high levels of PGK1 are a relevant factor for tumor growth, tumor progression and metastasis. Taken together, previously published *in-vitro* and recent *in-vivo* results suggest that PGK1 appears to be a crucial enzyme which enables gastric tumors to metastasize. Further, the assessment of tumor growth and metastasis by *in-vivo* PET/MR-imaging is a novel technique providing an excellent correlation between imaging results and histopathological findings. Additionally, our metastatic mouse model, simulating human gastric cancer, proved concordant concerning its behavior with aggressive gastric cancer in humans. In the future, further work will focus on assessing different treatment strategies in gastric cancer by novel imaging techniques and improving detection sensitivity down to marginal metastases. In synopsis, PGK1 might be a promising future therapeutical target in gastric cancer and MR and PET-MR-imaging constitute promising tools for prediction of tumor extent and therapy response *in-vivo*.

Abbreviations

ATP (Adenosine triphosphate); CT (computed tomography); CXCR4 (CXC motive chemokine receptor 4); [^{18}F]DG (fluorodeoxyglucose (^{18}F)); FOV (field of view); MBq (Megabecquerel); MR (magnetic

resonance); MKN45 (human gastric adenocarcinoma cell line (medullary type; poorly differentiated)); MRI (magnetic resonance imaging); PET (positron emission tomography); PGK1 (phosphoglycerate kinase 1); RPMI (Roswell Park Memorial Institute); T (Tesla); TE (echo time); TR (repetition time).

Acknowledgements

The authors gratefully acknowledge the input and contributions to the present study made by Isabel Tritschler, Melanie Hauth, Matthias Wingert, Asghar Abbasi and Russell S. Taichman.

References

1 Parkin DM, Pisani P, Ferlay J: Global cancer statistics. CA Cancer J Clin 1999;49:33-64.

2 Yasumoto K, Koizumi K, Kawashima A, Saitoh Y, Arita Y, Shinohara K, Minami T, Nakayama T, Sakurai H, Takahashi Y, Yoshie O, Saiki I: Role of the CXCL12/CXCR4 axis in peritoneal carcinomatosis of gastric cancer. Cancer Res 2006;66:2181-2187.

3 Bando E, Yonemura Y, Takeshita Y, Taniguchi K, Yasui T, Yoshimitsu Y, Fushida S, Fujimura T, Nishimura G, Miwa K: Intraoperative lavage for cytological examination in 1,297 patients with gastric carcinoma. Am J Surg 1999;178:256-262.

4 Gonzalez-Moreno S, Gonzalez-Bayon L, Ortega-Perez G, Gonzalez-Hernando C: Imaging of peritoneal carcinomatosis. Cancer J 2009;15:184-189.

5 Funicelli L, Travaini LL, Landoni F, Trifiro G, Bonello L, Bellomi M: Peritoneal carcinomatosis from ovarian cancer: the role of CT and [(18)F]FDG-PET/CT. Abdom Imaging 2009, in press.

6 Pfannenberg C, Konigsrainer I, Aschoff P, Oksuz MO, Zieker D, Beckert S, Symons S, Nieselt K, Glatzle J, Weyhern CV, Brucher BL, Claussen CD, Königsrainer A: (18)F-FDG-PET/CT to select patients with peritoneal carcinomatosis for cytoreductive surgery and hyperthermic intraperitoneal chemotherapy. Ann Surg Oncol 2009;16:1295-1303.

7 Antoch G, Bockisch A: Combined PET/MRI: a new dimension in whole-body oncology imaging? Eur J Nucl Med Mol Imaging 2009;36 Suppl 1:113-120.

8 Heiken JP: Contrast safety in the cancer patient: preventing contrast-induced nephropathy. Cancer Imaging 2008;8 Spec No A:124-127.

9 Zieker D, Konigsrainer I, Traub F, Nieselt K, Knapp B, Schillinger C, Stirnkorb C, Fend F, Northoff H, Kupka S, Brucher BL, Konigsrainer A: PGK1 a potential marker for peritoneal dissemination in gastric cancer. Cell Physiol Biochem 2008;21:429-436.

10 Wang J, Wang J, Dai J, Jung Y, Wei CL, Wang Y, Havens AM, Hogg PJ, Keller ET, Pienta KJ, Nor JE, Wang CY, Taichman RS: A glycolytic mechanism regulating an angiogenic switch in prostate cancer. Cancer Res 2007;67:149-159.

11 Daly EB, Wind T, Jiang XM, Sun L, Hogg PJ: Secretion of phosphoglycerate kinase from tumour cells is controlled by oxygen-sensing hydroxylases. Biochim Biophys Acta 2004;1691:17-22.

12 Duan Z, Lamendola DE, Yusuf RZ, Penson RT, Preffer FI, Seiden MV: Overexpression of human phosphoglycerate kinase 1 (PGK1) induces a multidrug resistance phenotype. Anticancer Res 2002;22:1933-1941.

13 Hwang TL, Liang Y, Chien KY, Yu JS: Overexpression and elevated serum levels of phosphoglycerate kinase 1 in pancreatic ductal adenocarcinoma. Proteomics 2006;6:2259-2272.

14 Zhang D, Tai LK, Wong LL, Chiu LL, Sethi SK, Koay ES: Proteomic study reveals that proteins involved in metabolic and detoxification pathways are highly expressed in HER-2/neu-positive breast cancer. Mol Cell Proteomics 2005;4:1686-1696.

15 Zieker D, Königsrainer I, Tritschler I, Löffler M, Beckert S, Traub F, Nieselt K, Bühler S, Weller M, Gaedcke J, Taichman RS, Northoff H, Brücher BL, Königsrainer A: Phosphoglycerate kinase 1 a promoting enzyme for peritoneal dissemination in gastric cancer. Int J Cancer 2010;126:1513-1520.

16 Hobbs S, Jitrapakdee S, Wallace JC: Development of a bicistronic vector driven by the human polypeptide chain elongation factor 1alpha promoter for creation of stable mammalian cell lines that express very high levels of recombinant proteins. Biochem Biophys Res Commun 1998;252:368-372.

17 Bhargava S, Hotz B, Buhr HJ, Hotz HG: An orthotopic nude mouse model for preclinical research of gastric cardia cancer. Int J Colorectal Dis 2009;24:31-39.

18 Warburg O: On respiratory impairment in cancer cells. Science 1956;124:269-270.

19 Judenhofer MS, Wehrl HF, Newport DF, Catana C, Siegel SB, Becker M, Thielscher A, Kneilling M, Lichy MP, Eichner M, Klingel K, Reischl G, Widmaier S, Röcken M, Nutt RE, Machulla HJ, Uludag K Cherry SR, Claussen CD, Pichler BJ: Simultaneous PET-MRI: a new approach for functional and morphological imaging. Nat Med 2008;14:459-465.